Magnetic fabrics and frictional behaviour of subduction zone input material from the erosive continental margin offshore Costa Rica (Costa Rica Seismogenesis Project, IODP expeditions 334 and 344)

ROBERT M. KURZAWSKI[1], MICHAEL STIPP[1], ANDRÉ NIEMEIJER[2], JENS C. GRIMMER[3], AGNES KONTNY[3], CHRISTOPHER J. SPIERS[2] AND JAN H. BEHRMANN[1]

[1]Department of Marine Geodynamics, GEOMAR Helmholtz Centre for Ocean Research Kiel, Kiel, Germany, (rkurzawski@geomar.de)
[2]HPT Laboratory, Faculty of Geosciences, Utrecht University, Utrecht, The Netherlands
[3]Institute of Applied Geosciences, Karlsruhe Institute of Technology (KIT), Karlsruhe, Germany

Introduction

There are two general types of continental subduction zones which form either accretionary or erosive margins. Along accretionary margins, the forearc wedge of the overriding continental plate grows by the accretion of material tectonically detached from the downgoing oceanic plate. Along erosive margins comprising slightly more than half of the active margins worldwide, the forearc wedge of the overriding continental plate shrinks due to tectonic erosion by the downgoing oceanic plate. Two major endeavors of the International Ocean Discovery Program (IODP), the Nankai Trough Seismogenic Zone Experiment (NanTroSEIZE) and the Costa Rica Seismogenesis Project (CRISP), investigate the processes and controlling factors of deformation and seismogenesis at accretionary and erosive continental margins including the incidence of megathrust earthquakes. In our project focussing on the Costa Rica erosive margin we want to understand the material properties which promote either distributed and continuous deformation or localized and discontinuous deformation in the forearc wedge. Our results will also be compared to similar investigations on sediments from the Nankai accretionary prism.

Offshore Costa Rica, the Cocos plate is subducted towards NE beneath the Caribbean plate at the Middle America Trench. IODP expeditions 334 and 344 drilled into the shallow upper Caribbean plate at the upper slope (U1379, U1413), midslope (U1378, U1380) and the lower trench slope (U1412). Additionally, the entire sedimentary sequence covering the incoming Cocos plate as well as the uppermost part of the magmatic oceanic basement have been penetrated at two drill sites (U1381, U1414). We have experimentally deformed a set of 7 samples from these locations in a rotary shear apparatus in order to determine their frictional behavior at relatively slow sliding velocity (1-100 µm/s). Results can be compared to experiments on sample material from an adjacent drillhole (ODP legs 170 and 205, Ikari et al., 2013) and from the Nankai accretionary prism (den Hartog et al., 2012). Such experiments improve our understanding of earthquake nucleation and propagation and the influence of external parameters and material properties. For the extensive characterization of the latter we have carried out laser diffraction particle size analysis, backscattered electron imaging, electron microprobe analysis and measurements of the low-field anisotropy of the magnetic susceptibility (AMS). The first results of our study will be presented under consideration of various shipboard data including density and porosity measurements.

Methods

Thirty-one IODP samples recovered from NanTroSEIZE (Exp 315, 316, 333, 338) and CRISP (Exp 344) expeditions were selected to investigate the AMS in a low magnetic field of 300 Am^{-1}. The AMS reveals the crystallographic preferred orientation (CPO) of paramagnetic minerals so that magnetic fabrics correlate to bulk CPO analysis. If ferrimagnetic minerals are absent or can be extracted from the data set, pervasive planar anisotropies like bedding and fault planes can be identified and even quantified. The method is in particular useful to study fabric development of fine-grained sediments, such as the clayey sediments sampled in NanTroSEIZE and CRISP expeditions. We have measured the AMS of 14 original CRISP samples from a depth down to 365 mbsf, 8 original NanTroSEIZE samples from a depth range of 28 to 522 m and 9 NanTroSEIZE samples experimentally deformed to variable strain conditions (Stipp et al., 2013). 15 of the 17 NanTroSEIZE samples used here were previously analyzed by synchrotron texture (=CPO) analysis (Schumann et al., subm). A comparison of the naturally compacted and experimentally deformed samples is used here to evaluate the effect of compaction and triaxial deformation on magnetic fabrics of weakly consolidated sediments. In total 126 cylindrical specimens with a diameter of 14 mm and a heigth of 12 mm were prepared from the 31 samples. Due to the lack of orientation data a part of the magnetic fabrics are only rotationally symmetric to the core axis.

The AMS was measured using a KLY-4S Kappabridge (AGICO) in a field of 300 Am^{-1} and a frequency of 875 Hz at room temperature. The SUFAR software package (AGICO) was used to calculate the principal susceptibilities with $K_{min} \leq K_{int} \leq K_{max}$ and the mean susceptibility K_{mean}. From these values the corrected degree of anisotropy P' and the shape factor T of the AMS ellipsoid can be derived (Jelinek, 1981). The shape of the ellipsoid is oblate if $0 < T \leq 1$ and prolate if $-1 \leq T < 0$. Primary sedimentary fabrics commonly exhibit P'-values < 1.1. Higher P´-values are characteristic for deformation fabrics. One sample exhibiting a suspiciously high mean susceptibility was tested for the presence of ferrimagnetic minerals measuring the temperature dependence of magnetic susceptibility (K(T)) between -194 and 700 °C.

Seven samples from 4 different CRISP drilling sites (U1379: upper slope, U1378: midslope, U1412: lower trench slope, U1414: incoming plate) were experimentally deformed in a hydrothermal rotary shear apparatus described by (Niemeijer et al., 2008). Remolded sample material of a grain size < 125 µm simulating a fault gouge was evenly distributed between the confining rings and the two opposing internal pistons usually resulting in an initial layer thickness of about 2 mm. Experimental conditions were defined to suitably cover the expected conditions at the CRISP updip limit of seismogenesis in approximately 5-6 km depth. Three experiments were conducted on each sample: one at room temperature and two at elevated temperatures of 70 °C and 140 °C. During tempered experiments the pore fluid pressure was held constant at 60 MPa and 120 MPa, respectively. In each experiment, the effective normal stress was increased in steps of 20 MPa from 30 MPa to 110 MPa. Shear strength and displacement were measured with a resolution of 0.2 MPa and 0.001 mm, respectively. At each of the applied normal stresses we performed an increasing velocity stepping to determine the velocity dependence of friction, quantified by the parameter $(a\text{-}b) = \Delta\mu/\ln V$ (e.g. (Marone et al., 1990). After reaching a steady state shear stress level during a first shear displacement of 1-3 mm at constant sliding velocity of 10 µm/s, sliding velocity was increased from 1 to 100 µm/s in half orders of magnitude. Assuming zero cohesion, the coefficient of sliding friction ($\mu = \tau/\sigma_n^{eff}$) was

calculated. The total displacement of a successful experiment adds up to 45 mm. Finite layer thickness was usually approximately 400 µm. The deformed sample material was impregnated with epoxy resin for later microstructural analysis.

Backscattered and secondary electron imaging was carried out using a JEOL JXA 8200 electron microprobe operated at a high Voltage of 20 kV and a low probe current of 1.4 nA in favour of a high imaging resolution. Intact CRISP samples were freeze dried and embedded in Araldite 2020 epoxy resin under vacuum to preserve the original pore space and microstructure. Ring-shaped experimental samples were cut tangentially, i.e. approximately parallel to the kinematic section.

Results

K_{mean}-values show a large variation ranging from 70 to 3700 x 10^{-6} SI units due to a heterogenous distribution of magnetite, which was identified based on a pronounced Verwey transition at -152 °C and a Curie temperature of 595 °C, revealed by temperature-dependent measurement of the susceptibility (K(T)). CRISP samples show lower K_{mean}-values than samples from the Nankai Trough (Fig. 1a,b; note the logarithmic scale). Experimentally deformed samples show the highest susceptibilies (Fig. 1c). In the absence of magnetite, magnetic fabrics of the clay-rich samples are controlled by the orientation of paramagnetic sheet silicates. The orientation of the principal susceptibility axes of the ferrimagnetic samples are coaxial with the paramagnetic samples. Nankai samples predominantly show oblate fabrics (Fig. 1b). Experimentally deformed samples consistently show oblate magnetic fabrics with T-values > 0.2 and P'-values of up to 1.15. Stereographic projections of the principal susceptibility axes nicely document the reorientation of platy sheet silicates into an orientation perpendicular to the axis of shortening. The concentration of K_{min} axes (red dots) in the center, and K_{int} and K_{max} axes on the periphery of the diagram can be interpreted as the formation of a new subhorizontal planar fabric (foliation). In contrast to the Nankai material, samples from the CRISP area show both, oblate and prolate magnetic fabrics. The prolate fabrics occur predominantly at the lower trench slope (U1412) possibly indicating superposition of two sub-fabrics.

The frictional behaviour of the investigated CRISP samples varies distinctly with lithological differences. Frictional records of two representative samples, each deformed at room temperature and at an elevated temperature, are exemplarily shown in Fig. 2. Sample 1414-30X7 is a nannofossil-rich calcareous ooze from the incoming plate. Consistent with a previous study (Ikari et al., 2013), frictional strength of this material is high at room temperature, where the apparent friction coefficient consistently shows values between 0.8 – 0.85 with little sensitivity to increasing stress, strain or sliding velocity (Fig. 2a). At 140 °C, however, a strong dependency on effective normal stress causes a significant weakening from values of about 0.9 at 30 MPa to 0.55 at 110 MPa. This "normal stress weakening" is accompanied by velocity weakening at medium velocity steps and unstable slip ("stick-slip" events). Unstable slip occurs more frequently and with larger stress drop amplitudes when effective normal stress is increased. This behaviour was previously considered as a possible trigger for earthquake nucleation at low temperatures beneath 120 °C at the Middle America Trench (Ikari et al., 2013). As in the geological record the active margin off Costa Rica repeatedly changed from tectonic erosion to accretion (e.g.(Vannucchi et al., 2001) it can be assumed that this incoming plate sediment might be incorporated into the subduction channel and the seismogenic zone in the future. Indeed, similar pelagic sediments have been found in the paleo-forearc and might contribute to seismogenesis with a similar unstable behavior.

Sample U1378-42X4 is a silt/siltstone from the midslope drill site on the Caribbean plate. The friction coefficient displays intermediate values between approximately 0.3 at room temperature and 0.5 at 70 °C and 30 MPa effective normal stress (Fig. 2b). At low normal stress up to 50 MPa, the material shows potentially unstable (i.e. velocity weakening) behaviour. At higher effective normal stress in excess of 70 MPa the frictional record is characterized by a slightly increasing friction coefficient towards higher normal stress, velocity strenghtening and a consistent strain hardening trend. This forearc material might enter the subduction channel by subduction erosion. Its velocity weakening behaviour at low normal stress might be important for rupture propagation at shallow levels and for earthquake nucleation at the updip end of the seismogenic zone.

The finite microstructures of the sheared sample exhibit a dense fabric and a considerably smaller grain size compared to the intact sediment cores indicating grain size reduction during deformation. A set of fractures with Riedel shear orientations demonstrates some shear localization within the clayey silts deformed at 70 °C. In contrast, at 140 °C the same material exhibits a rather homogeneous fabric indicating more distributed deformation.

Figures

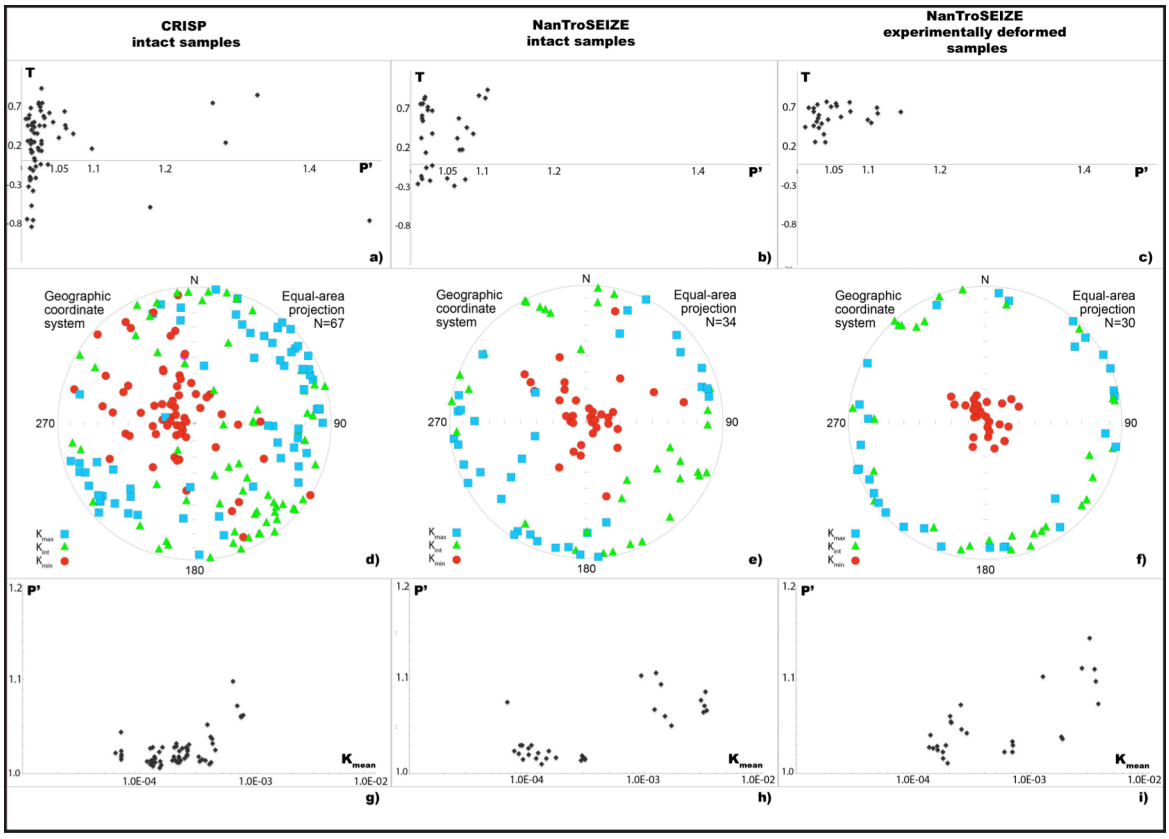

Figure 1: AMS data of Costa Rica (CRISP) and Nankai trench samples. T vs. P' plots show oblate and prolate magnetic fabrics for the CRISP samples (a) in contrast to triaxial and oblate fabrics for intact Nankai samples (b). Experimentally deformed samples exhibit stronger degrees of anisotropy and oblate magnetic fabrics (c). The formation of a new planar fabric is indicated by the reorientation of the principal susceptibility axes (f): K_{min} axes are oriented parallel to the axis of shortening. See text for further explanation.

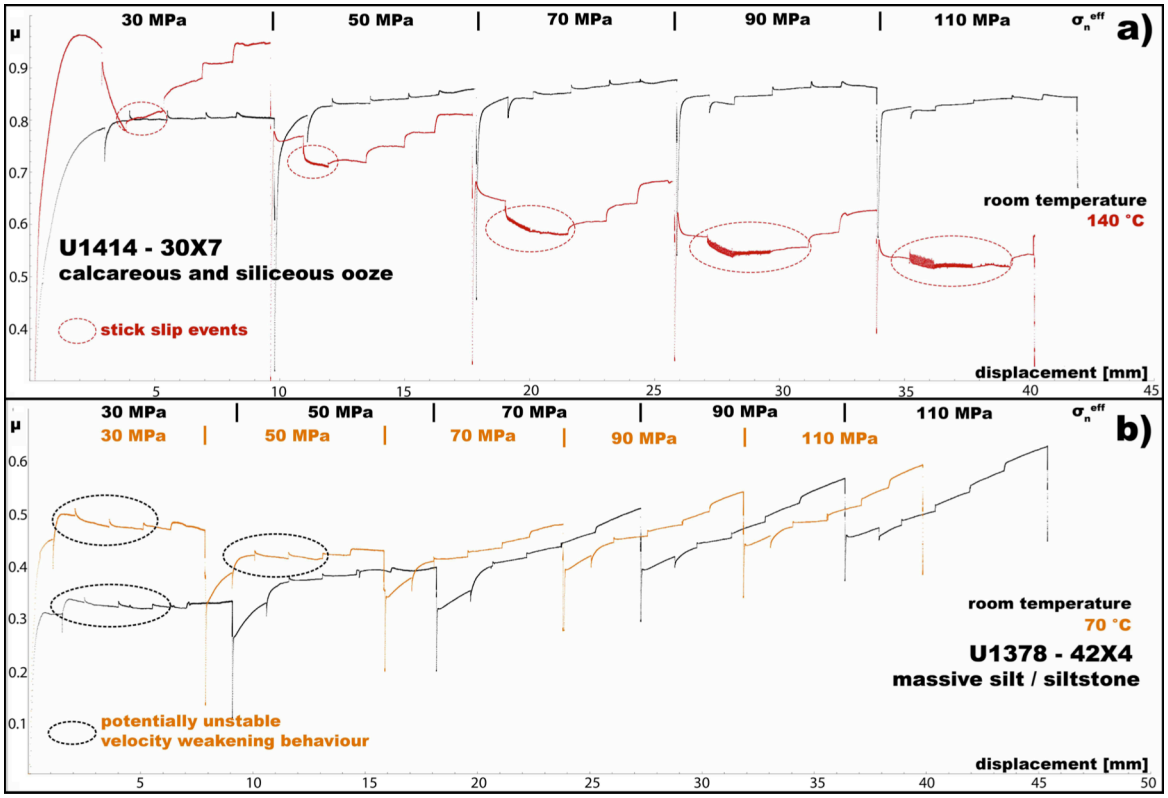

Figure 2.: Evolution of friction with shear displacement during velocity-stepping experiments at different temperatures on (a) calcareous ooze from the incoming plate (IODP site U1414) and (b) a clayey silt from the upper plate midslope drill site (U1378). At each applied effective normal stress velocity is stepped in the following order: 10-1-3-10-30-100 µm/s. See text for further explanations

References

den Hartog, den, S.A.M., Peach, C.J., de Winter, D.A.M., Spiers, C.J., and Shimamoto, T., 2012, Journal of Structural Geology, v. 38, p. 156–171.

Ikari, M.J., Niemeijer, A.R., Spiers, C.J., Kopf, A.J., and Saffer, D.M., 2013, Experimental evidence linking slip instability with seafloor lithology and topography at the Costa Rica convergent margin: Geology, v. 41, no. 8, p.891-894.

Jelinek, V., 1981, Tectonophysics, v. 79, p. T63–T67.

Marone, C., Raleigh, C.B., and Scholz, C.H., 1990, Journal of Geophysical Research: Solid Earth, v. 95, p. 7007–7025.

Niemeijer, Spiers, Peach, 2008, Tectonophysics, v. 460, p. 16–16.

Stipp, M., Rolfs, M., Kitamura, Y., Behrmann, J.H., Schumann, K., Schulte-Kortnack, D., and Feeser, V., 2013, Geochemistry, Geophysics, Geosystems, v. 14, p. 4791–4810.

Vannucchi, P., Scholl, D.W., Meschede, M., and McDougall Reid, K., 2001, Tectonics, v. 20, p. 649–668.